

Phonon-mediated electron attraction in SrTiO₃ via the generalized Fröhlich and deformation potential mechanisms

Norm M. Tubman,^{1,*} Christopher J. N. Coveney,² Chih-En Hsu,^{3,4} Andres Montoya-Castillo,⁵ Marina R. Filip,² Jeffrey B. Neaton,^{6,7,8} Zhenglu Li,⁴ Vojtech Vlcek,^{9,10} and Antonios M. Alvertis^{11,†}

¹NASA Ames Research Center, Moffett Field, California 94035, United States

²Department of Physics, University of Oxford, Oxford OX1 3PJ, United Kingdom

³Department of Physics, Tamkang University, New Taipei City 251301, Taiwan

⁴Mork Family Department of Chemical Engineering and Materials Science, University of Southern California, Los Angeles, California 90089, USA

⁵Department of Chemistry, University of Colorado Boulder, Boulder, CO 80309, USA

⁶Materials Sciences Division, Lawrence Berkeley National Laboratory, Berkeley, California 94720, United States

⁷Department of Physics, University of California Berkeley, Berkeley, California 94720, United States

⁸Kavli Energy NanoScience Institute at Berkeley, Berkeley, California 94720, United States

⁹Department of Chemistry and Biochemistry, University of California, Santa Barbara, CA 93106, USA

¹⁰Materials Department, University of California, Santa Barbara, CA 93106-9510, USA

¹¹KBR, Inc., NASA Ames Research Center, Moffett Field, California 94035, United States

(Dated: February 5, 2025)

Superconductivity in doped SrTiO₃ was discovered in 1964, the first superconducting transition observed in a doped semiconductor. However, the mechanism behind electron pairing in SrTiO₃ remains a subject of debate. By developing a theoretical framework to incorporate dynamical lattice screening in the electronic Coulomb interactions of semiconductors and insulators, we demonstrate analytically that long-range electron-phonon interactions described by a generalized multi-phonon Fröhlich mechanism result in phonon-mediated electron-electron attraction in SrTiO₃. Moreover, by combining our theory with first-principles calculations, we reveal an additional attractive interaction between electrons in SrTiO₃ due to the deformation potential mechanism, arising from the mixed ionic-covalent character of the Ti-O bond. Our results may have implications for the emergence of phonon-mediated electron attraction and superconductivity in a broader range of materials.

Introduction.— The prediction that doped semiconductors can exhibit phonon-mediated superconductivity was made in 1964 in the seminal works by Cohen [1, 2], leading to the discovery of superconductivity in doped SrTiO₃ in the same year [3]. Since then, superconductivity has been discovered in several semiconductors, including GeTe [4, 5], SnTe [6, 7], and MoS₂ [8]. Moreover, interfaces of SrTiO₃ with materials such as LaAlO₃ and LaTiO₃ exhibit superconductivity [9–11], generating interest in utilizing interface engineering to design high-temperature superconductors. Therefore, understanding the mechanism of SrTiO₃ superconductivity is a key step towards designing new types of superconductors.

To date, the precise mechanism of the pairing between electrons in SrTiO₃ remains elusive. As SrTiO₃ exhibits strong electron-phonon coupling [12, 13], several works have investigated the possibility of phonon-mediated superconductivity [1, 14–19]. Proposed mechanisms include inter-valley scattering [1, 14], coupling to polar [15], and defect [16] phonons, higher-order electron-phonon interactions [17], coupling to the soft infrared active zone-center phonon of SrTiO₃ [18], which is enhanced by anharmonic damping [20], and Rashba coupling [19, 21]. However, as also summarized in recent reviews [22, 23], the emergence of superconductivity through these mech-

anisms generally depends on adjustable parameters that are challenging to compute from first principles or to accurately infer from experiment. A fully first-principles explanation for the phonon-mediated electron-electron attraction remains elusive, as SrTiO₃ becomes superconducting at low doping densities where the Fermi energy is much smaller than the phonon frequencies, placing it in the non-adiabatic limit. As a result, the widely used Migdal-Eliashberg framework for phonon-mediated superconductivity does not apply [24], leading to an ongoing debate on the mechanism of Cooper pair formation.

Here we present a theory that rigorously incorporates lattice screening in electron-electron interactions. Without relying on adjustable parameters, we analytically demonstrate that linear electron-phonon coupling to multiple longitudinal optical (LO) phonons, alone is sufficient to yield long-range attraction between electrons in SrTiO₃. Moreover, we translate our theory to a first-principles computational scheme, and show that the deformation potential associated with vibrations of the Ti-O bond provides an additional strong, short-range attractive contribution to electron-electron interactions. Our theory, outlined in detail in our companion paper [25], applies to several doped semiconductors and insulators, and our predicted characteristics of the phonon-mediated electron attraction in SrTiO₃ are consistent with the qualitative features of its superconductivity.

Phonon-mediated electron-electron interactions— The density-density interaction between localized electronic

* norman.m.tubman@nasa.gov

† antoniosmarkos.alvertis@nasa.gov

states i, j , centered around lattice vectors \mathbf{R}, \mathbf{R}' , is [26]

$$U_{i\mathbf{R}j\mathbf{R}'}(\omega) = \int_V d\mathbf{r} \int_V d\mathbf{r}' \phi_{i\mathbf{R}}^*(\mathbf{r}) \phi_{i\mathbf{R}}(\mathbf{r}) W(\mathbf{r}, \mathbf{r}', \omega) \phi_{j\mathbf{R}'}^*(\mathbf{r}') \phi_{j\mathbf{R}'}(\mathbf{r}'). \quad (1)$$

Here $\phi_{i\mathbf{R}}(\mathbf{r})$ are a basis localized in real space, here maximally localized Wannier functions (MLWFs) [27]. Additionally, $W(\omega)$ is the frequency-dependent screened Coulomb interaction, which has two contributions: an electronically screened Coulomb interaction W^{el} , and a contribution from phonons. Within many-body perturbation theory and to the lowest order in the electron-phonon interaction, the phonon contribution to the screened Coulomb interaction is written as [28–30]

$$W^{ph}(\mathbf{r}, \mathbf{r}', \omega) = \sum_{\mathbf{q}, \nu} D_{\mathbf{q}, \nu}(\omega) g_{\mathbf{q}, \nu}(\mathbf{r}) g_{\mathbf{q}, \nu}^*(\mathbf{r}'). \quad (2)$$

Here $D_{\mathbf{q}, \nu}(\omega)$ is the propagator of a phonon with branch index ν at wavevector \mathbf{q} , and $g_{\mathbf{q}, \nu}$ is the electron-phonon vertex. The overall screened Coulomb interaction then becomes $W(\omega) = W^{el}(\omega) + W^{ph}(\omega)$. By inserting $W(\omega)$ into eq. (1), we obtain the total interaction term for electrons in localized states i, j , centered around \mathbf{R}, \mathbf{R}' respectively, as $U_{i\mathbf{R}j\mathbf{R}'}(\omega) = U_{i\mathbf{R}j\mathbf{R}'}^{el}(\omega) + U_{i\mathbf{R}j\mathbf{R}'}^{ph}(\omega)$.

Assuming an isotropic material with high-frequency dielectric constant ϵ_∞ and ignoring local field effects, the purely electronic part of the interaction in the static limit ($\omega = 0$) can be written in the intuitive form

$$U_{\mathbf{R}\mathbf{R}'}^{el, st} = \frac{1}{\epsilon_\infty |\mathbf{R} - \mathbf{R}'|}, \quad (3)$$

where we have suppressed the band index, and neglected the screening of the Coulomb interaction by free carriers in doped systems, which is justified given the low doping densities at which SrTiO₃ becomes superconducting. For the phonon-mediated interaction, as detailed in our companion paper [25], we obtain for periodic systems

$$\begin{aligned} U_{i\mathbf{R}j\mathbf{R}'}^{ph}(\omega) &= \langle \phi_{i\mathbf{R}} \phi_{j\mathbf{R}'} | W^{ph}(\omega) | \phi_{i\mathbf{R}} \phi_{j\mathbf{R}'} \rangle \\ &= \sum_{\mathbf{q}, \nu} g_{i\mathbf{q}\nu}(\mathbf{0}) g_{j\mathbf{q}\nu}^*(\mathbf{R}' - \mathbf{R}) \\ &\quad \times \left[\frac{1}{\omega - \omega_{\mathbf{q}, \nu} + i\delta} - \frac{1}{\omega + \omega_{\mathbf{q}, \nu} - i\delta} \right]. \end{aligned} \quad (4)$$

In the static limit, and for on-site ($\mathbf{R} = \mathbf{R}'$) intra-band ($i = j$) terms this becomes

$$U_{i\mathbf{R}i\mathbf{R}}^{ph, st} = -2 \sum_{\mathbf{q}\nu} \frac{|g_{i\mathbf{q}\nu}(\mathbf{0})|^2}{\omega_{\mathbf{q}, \nu}}, \quad (5)$$

which is a purely attractive interaction, in agreement with the conventional understanding of the effect of phonon screening on electron-electron interactions [31].

The superscript “*st*” denotes the static limit $\omega = 0$.

In polar semiconductors and insulators, long-range dipolar electron-phonon coupling dominates the electron-phonon interaction [32], and is written as

$$g_{i\mathbf{q}\nu}^{\mathcal{L}}(\mathbf{R}) = i \frac{4\pi}{V} \sum_{\kappa} \left(\frac{1}{2NM_{\kappa}\omega_{\mathbf{q}, \nu}} \right)^{1/2} \frac{\mathbf{q} \cdot \mathbf{Z}_{\kappa} \cdot \mathbf{e}_{\kappa\nu}}{\mathbf{q} \cdot \epsilon_\infty \cdot \mathbf{q}} \times \langle \phi_{i\mathbf{R}}(\mathbf{r}) | e^{i\mathbf{q} \cdot \mathbf{r}} | \phi_{j\mathbf{R}}(\mathbf{r}) \rangle, \quad (6)$$

which is the generalization of the Fröhlich model [33]. Here we ignore local field effects, *i.e.* we set $\mathbf{q} + \mathbf{G} \rightarrow \mathbf{q}$, where \mathbf{G} a reciprocal lattice vector. For an atom κ , M_{κ} and \mathbf{Z}_{κ} are its mass and Born effective charge tensor respectively, $\mathbf{e}_{\kappa\nu}$ a vibrational eigenvector, and ϵ_∞ the dielectric matrix tensor.

By using the expression of eq. (6) in the phonon-mediated electron-electron interaction of eq. (4), taking the static limit, and assuming an isotropic dielectric and dispersionless phonons, we obtain the expression

$$U_{\mathbf{R}\mathbf{R}'}^{ph, st, \mathcal{L}} = - \sum_{\nu} \frac{\omega_{LO, \nu}^2 - \omega_{TO, \nu}^2}{\omega_{LO, \nu}^2} \cdot \frac{1}{\epsilon_\infty |\mathbf{R} - \mathbf{R}'|}, \quad (7)$$

which is an attractive interaction, with the contribution of each LO mode being proportional to the splitting $\omega_{LO, \nu}^2 - \omega_{TO, \nu}^2$ from the corresponding transverse optical (TO) mode. This result is derived within our companion paper [25], alongside expressions for the general frequency-dependent case, which accounts for anisotropic dielectric and dispersive phonons. By comparing this expression to the repulsive electron-electron interaction of eq. (3), it is evident that an overall long-range attraction appears when $\sum_{\nu} \frac{\omega_{LO, \nu}^2 - \omega_{TO, \nu}^2}{\omega_{LO, \nu}^2} > 1$.

Before we proceed to discuss the specific results for SrTiO₃, it is worth highlighting the importance of using the generalized Fröhlich vertex of eq. (6) in deriving eq. (7), rather than the traditional Fröhlich expression

$$g_{\mathbf{q}}^{Fr}(\mathbf{r}) = \frac{i}{|\mathbf{q}|} \sqrt{\frac{4\pi}{NV} \frac{\omega_{LO}}{2} \left(\frac{1}{\epsilon_\infty} - \frac{1}{\epsilon_0} \right)} e^{i\mathbf{q} \cdot \mathbf{r}}, \quad (8)$$

where ϵ_0 the static dielectric constant. The assumptions that reduce eq. (6) to eq. (8) are that of taking the $\mathbf{q} \rightarrow 0$ limit for smoothly-varying quantities, having a band structure identical to that of the electron gas model, the permittivity being isotropic, and having only a single Einstein LO phonon [34]. Note however, that these assumptions are not valid for SrTiO₃. In the static limit, this yields the phonon-mediated electron attraction

$$U_{\mathbf{R}\mathbf{R}'}^{ph, st, Fr, \mathcal{L}} = - \left(\frac{1}{\epsilon_\infty} - \frac{1}{\epsilon_0} \right) \cdot \frac{1}{|\mathbf{R} - \mathbf{R}'|}. \quad (9)$$

This expression was used by Gor'kov [15] in an effort to explain the emergence of attractive electron-electron interactions in SrTiO₃. However, even in the extreme case of $\epsilon_0 \rightarrow \infty$, this will at best cancel out the repulsive

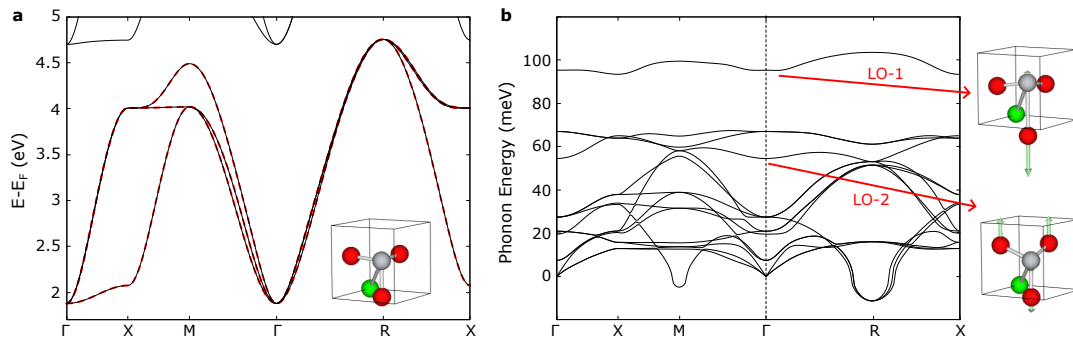


FIG. 1. Lowest conduction band manifold of SrTiO₃ computed at the DFT-LDA level (black) and using Wannier interpolation (red) in panel **a** (energies relative to valence band maximum). The inset visualizes the unit cell of the system (Sr: green, Ti: gray, O: red). Panel **b** shows the phonon dispersion as obtained within DFPT, alongside a visualization of the displacement patterns of the two highest frequency LO phonons.

ϵ_∞	ϵ_0	Z_{Sr}^*	Z_{Ti}^*	Z_{O}^{1*}	Z_{O}^{2*}	$\omega_{\text{TO}-1}, \omega_{\text{LO}-1}$ (meV)	$\omega_{\text{TO}-2}, \omega_{\text{LO}-2}$ (meV)	$\omega_{\text{TO}-3}, \omega_{\text{LO}-3}$ (meV)
6.2	587.6	2.56	7.25	-5.69	-2.05	67, 95	21, 54	7, 20

TABLE I. DFPT results for SrTiO₃: high- and low-frequency dielectric constants $\epsilon_\infty, \epsilon_0$, Born effective charges of different atoms (along two directions for oxygen), and frequencies of the pairs of TO, LO modes at Γ , for the three IR active LO phonons.

electron-electron Coulomb interaction of eq. (3), and cannot result in a net attraction [35]. This later led Gor'kov to hypothesize that electron coupling to defect phonons provides the missing additional attraction [16]. However, we see that our generalized expression of eq. (7), that does not rely on the aforementioned simplifications, provides a distinct answer: long-range electron-phonon coupling alone is sufficient to yield a strong attraction, once the effect of multiple LO phonons is accounted for fully.

Numerical results— SrTiO₃ exists in two phases. Above 105 K the system assumes a high-symmetry cubic perovskite structure, with perfectly aligned TiO₆ octahedra. The unit cell in this phase, shown in Fig. 1a, consists of a total of five atoms. Below 105 K the system is found in its tetragonal paraelectric phase [36, 37], where the TiO₆ octahedra undergo tilting, doubling the number of atoms in the unit cell. Here we focus on the cubic phase of SrTiO₃ due to the simpler character of its phonons and electron-phonon coupling, but note that our results, particularly on the impact of long-range electron-phonon coupling, may be generalized, as we elaborate below.

Fig. 1a shows the manifold of the first three conduction bands of SrTiO₃, as obtained within density functional theory (DFT) and the local density approximation (LDA). This follows an optimization of the unit cell at this level of theory, which results in real phonons at the zone center, as computed within density functional perturbation theory (DFPT), and visualized in Fig. 1b. The high degree of anharmonicity of cubic SrTiO₃ results in instabilities for zone boundary modes, at *R* and *M* in the Brillouin zone. However, these modes only provide minor electron-phonon coupling at low temperatures, and the remaining modes are in excellent agreement with previous calculations including anharmonicity [12]. Table I summarizes the DFPT results for the dielectric constants,

Born effective charges, and LO/TO mode frequencies of SrTiO₃. Since cubic SrTiO₃ has five atoms in its unit cell, there are four LO phonons, three of which are IR active, and the frequencies of these are given in Table I. Additionally, Fig. 1b illustrates the displacement patterns of the two highest frequency LO modes, which involve vibrations of the Ti-O bond. In Appendix A we provide computational details for all first-principles calculations.

We now visualize in Fig. 2a the Coulomb and long-range phonon-mediated electron-electron interactions of cubic SrTiO₃ according to equations (3) and (7). The phonon-mediated attraction (black) clearly overcomes the Coulomb repulsion (red) between electrons, resulting in a net attraction (blue). It is worth emphasizing that while we have used the simplified expression in eq. (7) here, even when using the generalized expression derived in our companion paper [25], where we maintain the phonon dispersion and allow for anisotropic dielectric response, the results are qualitatively identical. Importantly, one could also use the LO and TO mode frequencies of the tetragonal phase of SrTiO₃ as found in the literature [38] to evaluate the phonon-mediated attraction between electrons, which leads to $\sum_\nu \frac{\omega_{\text{LO},\nu}^2 - \omega_{\text{TO},\nu}^2}{\omega_{\text{LO},\nu}^2} > 1$, with specific values in the range of 2.2–2.6, which is very close to our value of 2.23 for this sum in the cubic phase, and in qualitative agreement in terms of the emergence of a net electron-electron attraction.

While eq. (7) allows us to evaluate the attractive interaction due to long-range electron-phonon coupling, other mechanisms have also been discussed as potentially playing a role in giving rise to attractive interactions, such as the deformation potential mechanism [18, 39]. In order to evaluate the relevance of such mechanisms to electron pairing in SrTiO₃, and due to the lack of analytic

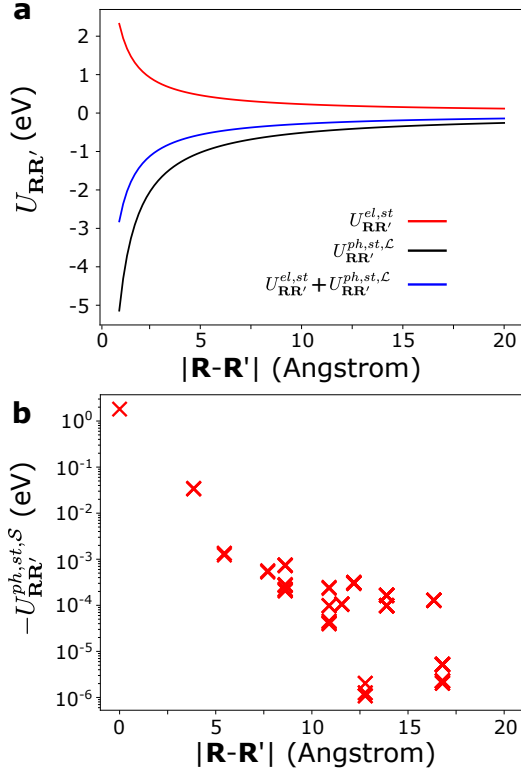


FIG. 2. Electron-electron Coulomb repulsion, phonon-mediated long-range electron attraction, and total interaction (panel a) as a function of distance between electrons. In panel b we visualize the phonon-mediated attraction as a function of distance due to short-range electron-phonon coupling.

expressions for general electron-phonon interactions, we return to eq. (4) and evaluate this term from first principles including only short-range electron-phonon coupling $g_{ii\mathbf{q}\nu}^S(\mathbf{R})$. Details of our first-principles implementation of eq. (4) are given in our companion paper [25]. Briefly, we use Quantum Espresso for DFT calculations [40], and Wannier90 [41] to produce MLWFs used as a basis for the terms in eqs. (1) and (4). The resulting MLWFs describing the conduction states of SrTiO₃ resemble Ti d orbitals, and yield a Wannier-interpolated band structure in excellent agreement with DFT (Fig. 1). We use RESPACK to evaluate the electronic Coulomb repulsion according to eq. (1) for the subspace of the three conduction states, within the constrained random phase approximation (cRPA) [42]. We use EPW [43], BerkeleyGW [44] and Abinit [45], allowing us to compute the phonon-mediated electron interaction following eq. (4) at the GW perturbation theory (GWPT) [46] level of theory.

Fig. 2b presents the spatial decay of the phonon-mediated attraction due to short-range electron-phonon coupling, in the static limit, with distance between conduction electrons. The most important contribution is to the on-site ($\mathbf{R} = \mathbf{R}'$) Coulomb term, where an attraction of $U_{\mathbf{R}\mathbf{R}}^{ph,st,S} = -1.858$ eV is found. Within cRPA we find that the on-site repulsion between two conduction

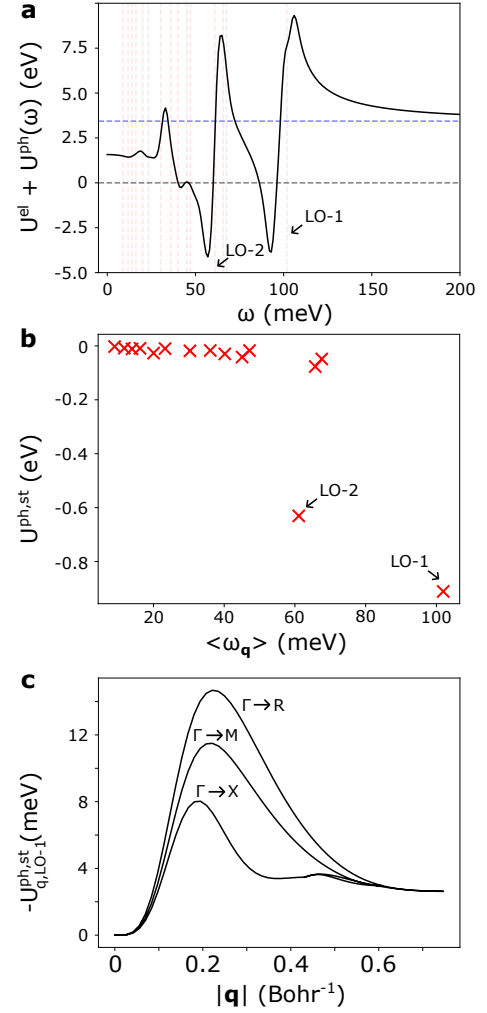


FIG. 3. On-site electron-electron interaction in SrTiO₃, mediated by short-range coupling to phonons. In panel a we plot the frequency dependence of the total interaction, where red lines are average phonon frequencies in the Brillouin zone, and the blue dashed line marks the static purely electronic interaction. In panel b we decompose the static on-site attraction to the contributions of different phonons, and panel c shows how the contribution of LO-1 depends on its momentum $|\mathbf{q}|$.

electrons is $U_{\mathbf{R}\mathbf{R}}^{el,st} = 3.436$ eV. Therefore, while there is a substantial reduction of 54% in the on-site Coulomb repulsion due to phonons, the overall interactions remains repulsive. Additionally, for $\mathbf{R} \neq \mathbf{R}'$ and nearest neighbors, the short-range electron-phonon interaction results in an attraction of $U_{\mathbf{R}\mathbf{R}'}^{ph,st,S} = -35$ meV, in addition to the one due to long-range coupling.

To better understand the attractive contribution from short-range electron-phonon coupling, we visualize in Fig. 3a the frequency dependence of the total on-site electron-electron interaction, including phonon effects. Here we have applied a Gaussian smoothing filter to reduce noise and emphasize the overall trend. We see that there are poles associated with the LO phonons, and it is only at fairly large frequencies of approximately

50 meV that the overall on-site interaction becomes attractive, although the precise frequency where this occurs can depend to some extent on the smoothing parameter. In Fig. 3b we visualize the contribution of individual phonons to the on-site phonon-mediated attraction in the static limit. This effect is dominated by the two highest frequency LO modes and we decompose the contribution of the highest frequency one (LO-1) along three high-symmetry paths in the Brillouin zone in Fig. 3c. We see that the absolute value of the phonon-mediated attraction initially grows with $|\mathbf{q}|$, and eventually peaks. This is consistent with analytic theories of electron-phonon coupling [32, 47], where the deformation potential includes octopole and higher-order terms, which vanish as $\mathbf{q} \rightarrow 0$.

Our results are consistent with the qualitative features of superconductivity in SrTiO₃. Despite the fact that on-site Coulomb interactions remain repulsive, solutions of the Hubbard model have shown that nearest neighbor and also longer-range attraction are sufficient to yield superconductivity [48–50]. Moreover, while electron doping will introduce carriers in the conduction bands and lead to Cooper pair formation, after a certain doping density the long-range electron-phonon interaction, which is the dominant mechanism of attraction, will be strongly screened [51], and eventually vanish. This is consistent with the dome-like behavior in the superconducting phase diagram of SrTiO₃ [23]. Our results are also consistent with the anomalous isotope effect of SrTiO₃, where superconductivity is enhanced upon substitution of ¹⁶O by ¹⁸O [52]. Oxygen substitution brings SrTiO₃ close to a phase transition into a ferroelectric phase, which reduces the frequency of the lowest TO mode [53], which in turn will increase the attraction between electrons mediated by the deformation potential coupling to this phonon, given the $1/\omega_{\mathbf{q},\nu}$ dependence of the phonon-mediated attraction U^{ph} . Moreover, we find that isotope substitution leads to minor changes of the sum $\sum_{\nu} \frac{\omega_{LO,\nu}^2 - \omega_{TO,\nu}^2}{\omega_{LO,\nu}^2}$, which suggests that the long-range mechanism is unaffected.

It is worth asking what makes SrTiO₃ special in terms of the emergence of strongly attractive electron-electron interactions, and whether similar behavior might be observed in other materials. As presented above, there are two mechanisms for phonon-mediated attraction at play. The first is the long-range coupling of electrons to multiple LO phonons. As expressed by eq. (7), this chan-

nel is significant in materials where multiple LO phonons have a substantial splitting from the corresponding TO phonons, which is a manifestation of large Born effective charges. The second contribution to a strong phonon-mediated electron attraction is the deformation potential mechanism, which is generally associated with strong covalent character of the bonds of a material [54]. As seen in Table I the Born effective charges of the Ti and O values are much greater than their nominal charges, reflecting the ionic-covalent character of the Ti-O bond, similar also to other cubic perovskites [55], and the dominant phonons are LO-1 and LO-2, which involve vibrations of Ti and O. A similar phonon-mediated attraction due to a deformation potential mechanism was found for GeTe in our companion paper [25], where strong mixed ionic-covalent character is also present.

Conclusions.—We have presented a theoretical framework for the phonon-mediated electron interactions of materials, and applied it to SrTiO₃. We have shown that long-range coupling of electrons to multiple LO phonons yields long-range electron-electron attraction, and we have derived a simple criterion to determine whether this is the case within a material. Moreover, we have combined our theory with first-principles calculations, and found a strong short-range phonon-mediated attraction of electrons, following a deformation potential mechanism, which is expected to be strong in systems with mixed ionic-covalent bonding. We expect that our theoretical and our computational framework will contribute towards a deeper understanding of phonon-mediated superconductivity in a wide range of materials.

Acknowledgments.—The authors are thankful to Marvin L. Cohen for helpful and inspiring discussions. This material is based upon work supported by the U.S. Department of Energy, Office of Science, National Quantum Information Science Research Centers, Superconducting Quantum Materials and Systems Center (SQMS) under contract No. DE-AC02-07CH11359. We are grateful for support from NASA Ames Research Center. VV was supported by the National Science Foundation (NSF) CAREER award through grant No. DMR-1945098. This research used resources of the National Energy Research Scientific Computing Center, a DOE Office of Science User Facility supported by the Office of Science of the U.S. Department of Energy under Contract No. DE-AC02-05CH11231 using NERSC awards HEP-ERCAP0029167 and DDR-ERCAP0029710.

[1] M. L. Cohen, Superconductivity in many-valley semiconductors and in semimetals, *Phys. Rev.* **134**, A511 (1964).
 [2] M. L. Cohen, The existence of a superconducting state in semiconductors, *Rev. Mod. Phys.* **36**, 240 (1964).
 [3] J. F. Schooley, W. R. Hosler, and M. L. Cohen, Superconductivity in Semiconducting SrTiO₃, *Phys. Rev. Lett.* **12**, 474 (1964).
 [4] M. Kriener, M. Sakano, M. Kamitani, M. S. Bahramy,

R. Yukawa, K. Horiba, H. Kumigashira, K. Ishizaka, Y. Tokura, and Y. Taguchi, Evolution of Electronic States and Emergence of Superconductivity in the Polar Semiconductor GeTe by Doping Valence-Skipping Indium, *Phys. Rev. Lett.* **124**, 047002 (2020).
 [5] H. Cheng, H. Yao, Y. Xu, J. Jiang, Y. Yang, J. Wang, X. Li, Y. Li, and J. Shao, Pressure-Induced Alloying and Superconductivity in GeTe, *Chemistry of Materials* **36**,

- 3764 (2024).
- [6] P. B. Allen and M. L. Cohen, Carrier-concentration-dependent superconductivity in SnTe and GeTe, *Phys. Rev.* **177**, 704 (1969).
 - [7] M. Novak, S. Sasaki, M. Kriener, K. Segawa, and Y. Ando, Unusual nature of fully gapped superconductivity in In-doped SnTe, *Phys. Rev. B* **88**, 140502 (2013).
 - [8] J. M. Lu, O. Zheliuk, I. Leermakers, N. F. Q. Yuan, U. Zeitler, K. T. Law, and J. T. Ye, Evidence for two-dimensional Ising superconductivity in gated MoS₂, *Science* **350**, 1353 (2015).
 - [9] S. Gariglio, N. Reyren, A. D. Caviglia, and J.-M. Triscone, Superconductivity at the LaAlO₃/SrTiO₃ interface, *Journal of Physics: Condensed Matter* **21**, 164213 (2009).
 - [10] J. Biscaras, N. Bergeal, A. Kushwaha, T. Wolf, A. Rastogi, R. C. Budhani, and J. Lesueur, Two-dimensional superconductivity at a Mott insulator/band insulator interface LaTiO₃/SrTiO₃, *Nature Communications* **1**, 10.1038/ncomms1084 (2010), [arXiv:1002.3737](https://arxiv.org/abs/1002.3737).
 - [11] S. Tan, Y. Zhang, M. Xia, Z. Ye, F. Chen, X. Xie, R. Peng, D. Xu, Q. Fan, H. Xu, J. Jiang, T. Zhang, X. Lai, T. Xiang, J. Hu, B. Xie, and D. Feng, Interface-induced superconductivity and strain-dependent spin density waves in FeSe/SrTiO₃ thin films, *Nature Materials* **12**, 634 (2013), [arXiv:1301.2748](https://arxiv.org/abs/1301.2748).
 - [12] J.-J. Zhou, O. Hellman, and M. Bernardi, Electron-Phonon Scattering in the Presence of Soft Modes and Electron Mobility in SrTiO₃ Perovskite from First Principles, *Phys. Rev. Lett.* **121**, 226603 (2018).
 - [13] G. Antonius, Y.-H. Chan, and S. G. Louie, Polaron spectral properties in doped ZnO and SrTiO₃ from first principles, *Phys. Rev. Res.* **2**, 043296 (2020).
 - [14] C. S. Koonce, M. L. Cohen, J. F. Schooley, W. R. Hosler, and E. R. Pfeiffer, Superconducting Transition Temperatures of Semiconducting SrTiO₃, *Phys. Rev.* **163**, 380 (1967).
 - [15] L. P. Gor'kov, Phonon mechanism in the most dilute superconductor n-type SrTiO₃, *Proceedings of the National Academy of Sciences* **113**, 4646 (2016).
 - [16] L. P. Gor'kov, Back to Mechanisms of Superconductivity in Low-Doped Strontium Titanate, *Journal of Superconductivity and Novel Magnetism* **30**, 845 (2017).
 - [17] Z. Han, S. A. Kivelson, and P. A. Volkov, Quantum bipolaron superconductivity from quadratic electron-phonon coupling, *Phys. Rev. Lett.* **132**, 226001 (2024).
 - [18] P. Wölfle and A. V. Balatsky, Superconductivity at low density near a ferroelectric quantum critical point: Doped SrTiO₃, *Phys. Rev. B* **98**, 104505 (2018).
 - [19] M. N. Gastiasoro, M. E. Temperini, P. Barone, and J. Lorenzana, Generalized rashba electron-phonon coupling and superconductivity in strontium titanate, *Phys. Rev. Res.* **5**, 023177 (2023).
 - [20] C. Setty, M. Baggioli, and A. Zaccane, Superconducting dome in ferroelectric-type materials from soft mode instability, *Phys. Rev. B* **105**, L020506 (2022).
 - [21] S. K. Saha, M. N. Gastiasoro, J. Ruhman, and A. Klein, *Strong Coupling Theory of Superconductivity and Ferroelectric Quantum Criticality in metallic SrTiO₃* (2024), [arXiv:2412.05374 \[cond-mat.str-el\]](https://arxiv.org/abs/2412.05374).
 - [22] C. Collignon, X. Lin, C. W. Rischau, B. Fauqué, and K. Behnia, Metallicity and Superconductivity in Doped Strontium Titanate, *Annual Review of Condensed Matter Physics* **10**, 25 (2019).
 - [23] M. N. Gastiasoro, J. Ruhman, and R. M. Fernandes, Superconductivity in dilute SrTiO₃: A review, *Annals of Physics* **417**, 168107 (2020).
 - [24] E. R. Margine and F. Giustino, Anisotropic migdaliashberg theory using wannier functions, *Phys. Rev. B* **87**, 024505 (2013).
 - [25] N. M. Tubman, C. J. N. Coveney, C.-E. Hsu, A. Montoya-Castillo, M. R. Filip, J. B. Neaton, Z. Li, V. Vlcek, and A. M. Alvertis, *Theory of ab initio downfolding with arbitrary range electron-phonon coupling* (2025), [arXiv:2502.00103 \[cond-mat.mtrl-sci\]](https://arxiv.org/abs/2502.00103).
 - [26] K. Nakamura, Y. Yoshimoto, Y. Nomura, T. Tadano, M. Kawamura, T. Kosugi, K. Yoshimi, T. Misawa, and Y. Motoyama, RESPACK: An ab initio tool for derivation of effective low-energy model of material, *Computer Physics Communications* **261**, 107781 (2021), [arXiv:2001.02351](https://arxiv.org/abs/2001.02351).
 - [27] N. Marzari, A. A. Mostofi, J. R. Yates, I. Souza, and D. Vanderbilt, Maximally localized wannier functions: Theory and applications, *Rev. Mod. Phys.* **84**, 1419 (2012).
 - [28] G. Baym, Field-theoretic approach to the properties of the solid state, *Annals of Physics* **14**, 10.1006/aphy.2000.6009 (1961).
 - [29] L. Hedin, New Method for Calculating the One-Particle Green's Function with Application to the Electron-Gas Problem, *Physical Review* **139**, 796 (1965).
 - [30] F. Giustino, Electron-phonon interactions from first principles, *Reviews of Modern Physics* **89**, 1 (2017).
 - [31] G. D. Mahan, *Many-Particle Physics*, Physics of Solids and Liquids (Springer, 2013).
 - [32] P. Vogl, Microscopic theory of electron-phonon interaction in insulators or semiconductors, *Phys. Rev. B* **13**, 694 (1976).
 - [33] C. Verdi and F. Giustino, Fröhlich electron-phonon vertex from first principles, *Physical Review Letters* **115**, 1 (2015), 1510.06373.
 - [34] W. H. Sio and F. Giustino, Unified ab initio description of fröhlich electron-phonon interactions in two-dimensional and three-dimensional materials, *Phys. Rev. B* **105**, 115414 (2022).
 - [35] J. Ruhman and P. A. Lee, Superconductivity at very low density: The case of strontium titanate, *Phys. Rev. B* **94**, 224515 (2016).
 - [36] R. Cowley, W. Buyers, and G. Dolling, Relationship of normal modes of vibration of strontium titanate and its antiferroelectric phase transition at 110°k, *Solid State Communications* **7**, 181 (1969).
 - [37] Y. Yamada and G. Shirane, Neutron Scattering and Nature of the Soft Optical Phonon in SrTiO₃, *Journal of the Physical Society of Japan* **26**, 396 (1969), <https://doi.org/10.1143/JPSJ.26.396>.
 - [38] T. TADANO and S. TSUNEYUKI, Ab initio prediction of structural phase-transition temperature of SrTiO₃ from finite-temperature phonon calculation, *Journal of the Ceramic Society of Japan* **127**, 404 (2019).
 - [39] J. Ruhman and P. A. Lee, Comment on "Superconductivity at low density near a ferroelectric quantum critical point: Doped SrTiO₃", *Phys. Rev. B* **100**, 226501 (2019).
 - [40] P. Giannozzi, S. Baroni, N. Bonini, M. Calandra, R. Car, C. Cavazzoni, D. Ceresoli, G. L. Chiarotti, M. Cococcioni, I. Dabo, A. Dal Corso, S. Fabris, G. Fratesi, S. de Gironcoli, R. Gebauer, U. Gerstmann, C. Gougoussi, A. Kokalj, M. Lazzeri, L. Martin-Samos, N. Marzari,

- F. Mauri, R. Mazzarello, S. Paolini, A. Pasquarello, L. Paulatto, C. Sbraccia, S. Scandolo, G. Sclauzero, A. P. Seitsonen, A. Smogunov, P. Umari, and R. M. Wentzcovitch, QUANTUM ESPRESSO: a modular and open-source software project for quantum simulations of materials, *Journal of Physics: Condensed Matter* **21**, 395502 (2009).
- [41] G. Pizzi, V. Vitale, R. Arita, S. Blügel, F. Freimuth, G. Géranton, M. Gibertini, D. Gresch, C. Johnson, T. Koretsune, J. Ibanez-Azpiroz, H. Lee, J. M. Lihm, D. Marchand, A. Marrazzo, Y. Mokrousov, J. I. Mustafa, Y. Nohara, Y. Nomura, L. Paulatto, S. Poncé, T. Ponweiser, J. Qiao, F. Thöle, S. S. Tsirkin, M. Wierzbowska, N. Marzari, D. Vanderbilt, I. Souza, A. A. Mostofi, and J. R. Yates, Wannier90 as a community code: New features and applications, *Journal of Physics Condensed Matter* **32**, 10.1088/1361-648X/ab51ff (2020).
- [42] F. Aryasetiawan, M. Imada, A. Georges, G. Kotliar, S. Biermann, and A. I. Lichtenstein, Frequency-dependent local interactions and low-energy effective models from electronic structure calculations, *Phys. Rev. B* **70**, 195104 (2004).
- [43] H. Lee, S. Poncé, K. Bushick, S. Hajinazar, J. Lafuente-Bartolome, J. Leveillee, C. Lian, J.-M. Lihm, F. Macheda, H. Mori, H. Paudyal, W. H. Sio, S. Tiwari, M. Zacharias, X. Zhang, N. Bonini, E. Kioupakis, E. R. Margine, and F. Giustino, Electron-phonon physics from first principles using the EPW code, *npj Computational Materials* **9**, 156 (2023).
- [44] J. Deslippe, G. Samsonidze, D. A. Strubbe, M. Jain, M. L. Cohen, and S. G. Louie, BerkeleyGW: A massively parallel computer package for the calculation of the quasiparticle and optical properties of materials and nanostructures, *Computer Physics Communications* **183**, 1269 (2012), 1111.4429.
- [45] X. Gonze, B. Amadon, G. Antonius, F. Arnardi, L. Baguet, J.-M. Beuken, J. Bieder, F. Bottin, J. Bouchet, E. Bousquet, N. Brouwer, F. Bruneval, G. Brunin, T. Cavignac, J.-B. Charraud, W. Chen, M. Côté, S. Cottenier, J. Denier, G. Geneste, P. Ghosez, M. Giantomassi, Y. Gillet, O. Gingras, D. R. Hamann, G. Hautier, X. He, N. Helbig, N. Holzwarth, Y. Jia, F. Jollet, W. Lafargue-Dit-Hauret, K. Lejaeghere, M. A. L. Marques, A. Martin, C. Martins, H. P. C. Miranda, F. Naccarato, K. Persson, G. Petretto, V. Planes, Y. Pouillon, S. Prokhorenko, F. Ricci, G.-M. Rignanese, A. H. Romero, M. M. Schmitt, M. Torrent, M. J. van Setten, B. Van Troeye, M. J. Verstraete, G. Zérah, and J. W. Zwanziger, The Abinit project: Impact, environment and recent developments, *Computer Physics Communications* **248**, 107042 (2020).
- [46] Z. Li, G. Antonius, M. Wu, F. H. da Jornada, and S. G. Louie, Electron-Phonon Coupling from Ab Initio Linear-Response Theory within the GW Method: Correlation-Enhanced Interactions and Superconductivity in $\text{Ba}_{1-x}\text{K}_x\text{BiO}_3$, *Phys. Rev. Lett.* **122**, 186402 (2019).
- [47] P. Lawaetz, Long-wavelength phonon scattering in non-polar semiconductors, *Phys. Rev.* **183**, 730 (1969).
- [48] M. Jiang, Enhancing d -wave superconductivity with nearest-neighbor attraction in the extended Hubbard model, *Phys. Rev. B* **105**, 024510 (2022).
- [49] C. Peng, Y. Wang, J. Wen, Y. S. Lee, T. P. Devereaux, and H.-C. Jiang, Enhanced superconductivity by near-neighbor attraction in the doped extended Hubbard model, *Phys. Rev. B* **107**, L201102 (2023).
- [50] W.-C. Chen, Y. Wang, and C.-C. Chen, Superconducting phases of the square-lattice extended Hubbard model, *Phys. Rev. B* **108**, 064514 (2023).
- [51] F. Macheda, P. Barone, and F. Mauri, Electron-phonon interaction and longitudinal-transverse phonon splitting in doped semiconductors, *Phys. Rev. Lett.* **129**, 185902 (2022).
- [52] A. Stucky, G. W. Scheerer, Z. Ren, D. Jaccard, J.-M. Poumirol, C. Barreteau, E. Giannini, and D. van der Marel, Isotope effect in superconducting n-doped SrTiO_3 , *Scientific Reports* **6**, 37582 (2016).
- [53] J. M. Edge, Y. Kedem, U. Aschauer, N. A. Spaldin, and A. V. Balatsky, Quantum Critical Origin of the Superconducting Dome in SrTiO_3 , *Phys. Rev. Lett.* **115**, 247002 (2015).
- [54] M. L. Cohen and S. G. Louie, *Fundamentals of Condensed Matter Physics* (Cambridge University Press, 2016).
- [55] W. Zhong, R. D. King-Smith, and D. Vanderbilt, Giant LO-TO splittings in perovskite ferroelectrics, *Phys. Rev. Lett.* **72**, 3618 (1994).
- [56] D. R. Hamann, Optimized norm-conserving Vanderbilt pseudopotentials, *Physical Review B - Condensed Matter and Materials Physics* **88**, 1 (2013), 1306.4707.
- [57] M. J. van Setten, M. Giantomassi, E. Bousquet, M. J. Verstraete, D. R. Hamann, X. Gonze, and G. M. Rignanese, The PSEUDODOJO: Training and grading a 85 element optimized norm-conserving pseudopotential table, *Computer Physics Communications* **226**, 39 (2018), arXiv:1710.10138.
- [58] Y. Zhang, J. Sun, J. P. Perdew, and X. Wu, Comparative first-principles studies of prototypical ferroelectric materials by LDA, GGA, and SCAN meta-GGA, *Phys. Rev. B* **96**, 035143 (2017).

Appendix A: Computational details

We employ Quantum Espresso [40] for DFT and DFPT calculations, Wannier90 [41] to generate the Wannier representation of the active space of the three SrTiO_3 conduction bands, and EPW [43] in order to perform Wannier-Fourier interpolation of electron-phonon matrix elements. We use scalar-relativistic optimized norm-conserving Vanderbilt pseudopotentials (ONCV) [56] with standard accuracy, taken from Pseudo Dojo [57]. Specifically, these include three valence electrons for Sr, four valence electrons for Ti, and two valence electrons for O.

Here we work within the local density approximation (LDA) of DFT, which is known to yield stable Γ phonons for SrTiO_3 [58]. We use a plane wave cutoff of 90 Ry. For cRPA calculations we compute the electronic density on a $6 \times 6 \times 6$ Γ -centered \mathbf{k} -grid, and we include 600 bands, using a cutoff of 20 Ry, and having excluded the three lowest-lying conduction bands as discussed in the main part of the manuscript. For DFPT and GWPT calculations we use an electronic density computed on a $6 \times 6 \times 6$ half-shifted \mathbf{k} -grid, and we obtain the phonons on

a $6 \times 6 \times 6$ grid of \mathbf{q} -points. We interpolate the phonon frequencies and electron-phonon matrix elements on a $20 \times 20 \times 20$ \mathbf{q} -grid, which is sufficient to converge the values for the phonon-mediated attractive contribution to the Coulomb interactions within the conduction bands, due to short-range electron-phonon coupling.

It is worth highlighting that GWPT calculations are known to yield more accurate, and often stronger electron-phonon interactions compared to DFPT [46].

Indeed we found for SrTiO_3 that using GWPT increases the absolute value of the short-range on-site correction to the Coulomb interaction due to phonons by 18%, compared to DFPT. However, there is no noticeable difference between the two for nearest neighbor interactions or beyond. Therefore, the interpretation of our results for the deformation potential mechanism does not rely on the specific level of theory that was used.